IOPscience iopscience.iop.org

Home Search Collections Journals About Contact us My IOPscience

X-ray scattering, dislocations and orthorhombic GaSb

This article has been downloaded from IOPscience. Please scroll down to see the full text article.

2000 J. Phys.: Condens. Matter 12 4747

(http://iopscience.iop.org/0953-8984/12/22/307)

View the table of contents for this issue, or go to the journal homepage for more

Download details:
IP Address: 171.66.16.221
The article was downloaded on 16/05/2010 at 05:10

Please note that terms and conditions apply.

J. Phys.: Condens. Matter **12** (2000) 4747–4756. Printed in the UK PII: S0953-8984(00)08183-2

X-ray scattering, dislocations and orthorhombic GaSb

A Yu Babkevich†, R A Cowley†, N J Mason† and A Stunault‡

† Clarendon Laboratory, Oxford University, Parks Road, Oxford OX1 3PU, UK
‡ XMaS, ESRF, BP220, 38043 Grenoble Cédex, France

Received 28 September 1999, in final form 31 March 2000

Abstract. The structure of two GaSb layers, 13 nm and 327 nm thick, grown by metal–organic vapour-phase epitaxy on a GaAs(001) substrate have been studied by means of high-resolution x-ray diffraction. The large lattice mismatch is largely relaxed by regular arrays of 90° dislocations. The results show that both layers have orthorhombic crystal structure, and provide detailed quantitative information about the distortions caused by the dislocations in both the GaSb layers and the GaAs substrate.

1. Introduction

The growth of high-quality epitaxial thin layers on convenient substrates is a crucial aspect of many technologies. There is usually a mismatch of the lattice parameters between the substrate and the layer and so strain is produced at the interface and this must be controlled to obtain high-quality thin layers. GaSb layers grown on the (001) planes of GaAs substrates are model systems for studying the growth of semiconducting layers and are convenient substrates for the growth of GaSb/InAs superlattices and, hence, infra-red detectors. The structure of the GaSb layers grown either by MBE or by MOVPE has been extensively studied with electron microscopy (TEM or HRTEM) [1–12]. In contrast, we have used high-resolution x-ray scattering techniques to study these layers and this paper reports on the complementary information obtained from x-ray scattering and atomic force microscopy (AFM).

The lattice mismatch between GaSb and GaAs is large, 7.8%, and so the critical thickness before the onset of dislocations to relieve the strain will be only a few if any monolayers. Electron microscopy has established that GaSb films with an average thickness less than 5–10 nm are discontinuous and consist of isolated islands [7, 12]. The GaSb grows as islands up to thicknesses of about 30–50 nm with lattice parameters close to those of bulk GaSb, $a_f = 0.609\,54$ nm. When layers are grown with a thickness of more than 50–80 nm the GaSb forms a continuous film, and the growth becomes two dimensional [3, 12]. For all thicknesses of the films the GaSb is almost completely relaxed and the residual strain in the layers is only about 0.3–0.6% [3, 13].

HRTEM has shown that the lattice parameter difference between the GaAs substrate and GaSb is relaxed by regular arrays of Lomer dislocations (90° misfit dislocations) with Burgers vectors in the plane of the GaAs/GaSb interface and line directions [110] and $[1\bar{1}0]$ [2, 3, 6–10, 13]. The creation of regular arrays of Lomer dislocations appears to be directly related to the 3D growth [8]. In contrast, 60° dislocations are believed to be created when the islands coalesce [4, 7], with growth of big islands of irregular shape [10] or growth at relatively high (>540 °C) temperatures [5]. The measured spacing of the Lomer dislocations,

D, is typically 5.4–5.8 nm [1–3, 6–10], consistent with what would be expected if most of the misfit was accommodated by these arrays of Lomer-type misfit dislocations. If most of the strain was relieved by 60° dislocations, the expected average dislocation spacing required would be about $D/2$, i.e. 2.75 nm.

The results of our x-ray scattering measurements are consistent with these previous investigations [1–5] and in addition the high resolution of the x-ray technique has enabled us to determine new features including the following:

(i) that the crystallographic structure of the layers is orthorhombic even for a 327 nm layer,
(ii) the degree of perfection of the lattice of Lomer dislocations,
(iii) that the 90° dislocations are located precisely at the interface and give rise to distortions of both the GaSb layer and of the GaAs buffer layer,
(iv) that the scattering changes from being characteristic of islands to that characteristic of a mosaic crystal as the thickness increases.

These results demonstrate the power of high-resolution x-ray scattering techniques for characterizing thin layers and the way they provide quantitative information about the dislocations complementary to that obtained from electron microscopy.

2. Experiments

The layers were grown using the MOVPE growth reactor at the Clarendon Laboratory in Oxford [14]. Si-doped semi-insulating, (001)-oriented, GaAs slices were used as substrates. The growth temperature was 520 °C and the growth rate was typically 1 μm h^{-1}. Initially 1 μm of GaAs was grown on the substrate and then layers of GaSb of different thicknesses were grown by varying the growth time appropriately. A thin layer (*sample A*) was grown for 40 s and a thicker layer (*sample B*) was grown for 1920 s; see table 1. Most of the x-ray scattering measurements were performed at the XMaS beamline (BM28) at the ESRF. A four-circle diffractometer was used in a vertical scattering plane with the x-ray wavelength chosen to be 0.112 716 nm. The resolution of the instrument was typically better than 2.5×10^{-3} nm^{-1} in the scattering plane and 0.36 nm^{-1} perpendicular to the scattering plane. The growth direction [001] was perpendicular to the surface of the sample and the samples were mounted with one of the ⟨110⟩ directions perpendicular to the scattering plane. The measurements were made in

Table 1. Properties of the samples.

Measured and calculated parameters	A	B
Mosaic spread (deg)	0.017	0.19
Layer thickness (nm)	13(1)	327(30)
Growing time in MOVPE reactor (s)	40	1920
Growing temperature (°C)	520	520
Lattice constant $a_\perp$ (nm)	0.61161	0.61039
Lattice constant a_{110} (nm)	0.42774	0.43019
Lattice constant $a_{1\bar{1}0}$ (nm)	0.43037	0.43084
Uniform strain in [001] $\epsilon_\perp$ (%)	0.36	0.14
Uniform strain in [110] $\varepsilon_{\parallel}$ (%)	−0.76	−0.19
Uniform strain in [$1\bar{1}0$] $\varepsilon_{\parallel}$ (%)	−0.15	−0.04
Spacing between satellites k_{110} (nm^{-1})	1.024(3)	1.091(4)
Spacing between satellites $k_{1\bar{1}0}$ (nm^{-1})	1.105(2)	1.129(1)
D_{110} (nm)	6.134(18)	5.756(20)
$D_{1\bar{1}0}$ (nm)	5.688(10)	5.565(5)

the Q_z–Q_x scattering plane where the Q_z-vector was along the [001] growth direction and Q_x was either along the [110] or [$1\bar{1}0$] direction in reciprocal space. The reciprocal-space units are given in nm^{-1}. In this system of coordinates the positions of the Bragg peaks are given in terms of two wave-vector-transfer components $q_x = |Q_x| = 2\pi/d_{\langle 110\rangle}$ and $q_z = |Q_z| = 2\pi/d_{001}$, and scans varying the wave-vector transfer along Q_z are called longitudinal scans and those varying it along Q_x are called transverse scans. For convenience, Bragg reflections will usually be given by conventional triple Miller indices HKL rather than by their (q_x, q_z) coordinates. The thickness of sample B was determined by extrapolation to $q_z = 0$ of the full width at half-maximum (FWHM) in q_z of the $(00L)$ reflections and was 327 ± 30 nm. The thickness of sample A was determined much more accurately from the distance between the thickness (Pendellösung) fringes surrounding the Bragg peaks in scans along the [001] direction and was 13 ± 1 nm, whereas the layer thickness expected from the growth time is only 6.8 nm. The discrepancy arises because this layer consists of islands, as shown by atomic force microscopy (AFM), figure 1, and the thickness deduced from the x-ray measurements corresponds to the average height of the islands. The ratio of the two thicknesses indicates that only about half of the substrate is covered by the islands.

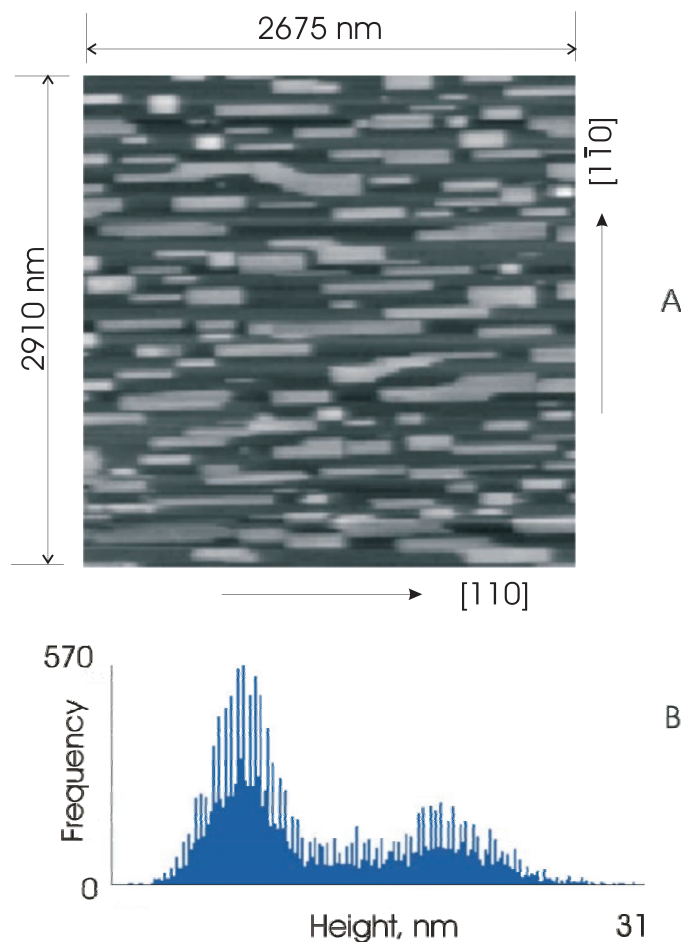

Figure 1. An AFM image from sample A.

3. Scattering from 90° misfit dislocations

Figure 2 shows the scattered intensity when the wave-vector transfer was scanned through the (002) Bragg reflection ($q_x = 0$, q_z) along the $[1\bar{1}0]$ direction, i.e. keeping q_z constant. The results for sample B (figure 2) show an intense Bragg peak from the bulk of the layer centred at ($q_x = 0$, q_z) and a regular series of satellite peaks at wave vectors with the same q_z and $q_x = \pm n \times 1.129(1)$ nm^{-1} (where n is an integer). The satellite peaks in figure 2(a) are the scattering from a regular array of 90° misfit dislocations. The wave vectors of the peaks give the separation between the dislocations D as 5.565(5) nm; see table 1. If the whole of the misfit strain were relieved by 90° misfit dislocations, the spacing $|\boldsymbol{b}|/f$ would be 5.5095 nm, where $f = (a_f - a_s)/a_s$ is the lattice mismatch and the Burgers vector $\boldsymbol{b} = \pm(1/2)\langle 1\bar{1}0\rangle$. If the strain was fully relieved by 60° dislocations, the spacing would be 2.755 nm, i.e. much

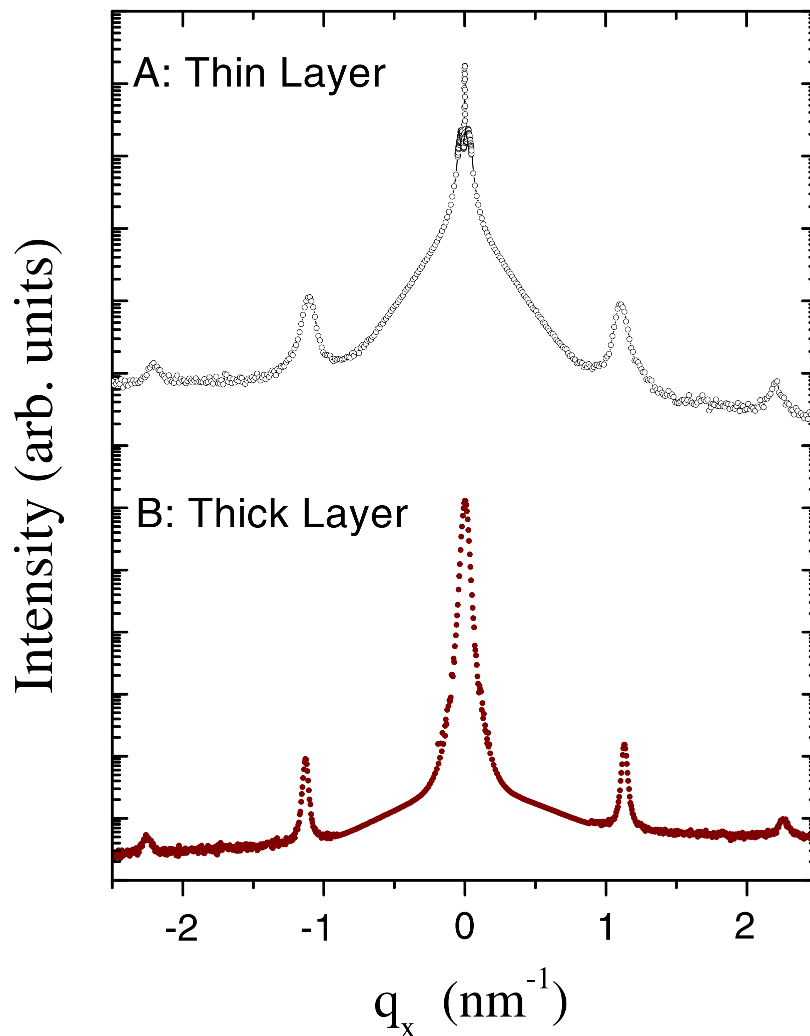

Figure 2. The x-ray scattering from transverse scans through the (002) Bragg reflections for GaSb for samples A and B. The wave vector q_x is parallel to the $[1\bar{1}0]$ direction.

smaller than the observed spacing. The widths of the satellite peaks increase with the peak index and, for example, are 0.032(2) nm^{-1} for the first-order ($n = 1$) satellites of the (002) Bragg reflections and 0.069(2) nm^{-1} for the second-order ($n = 2$) satellites. This increase in the width shows that there is cumulative disorder in the spacing of the dislocations, i.e. the variation of the spacing, which will then alter the positions of all subsequent dislocations in a dislocation array. Analysis similar to that of [15] suggests that the disorder in the position of the dislocations has a full width of 0.16 nm.

When sample B was rotated such that the [110] direction was in the scattering plane, the results were qualitatively similar but different in detail. The spacing of the satellites was different, 1.092(4) nm^{-1}, and corresponds to a distance between the dislocations of 5.754(21) nm. This is larger than the spacing in the $[1\bar{1}0]$ direction showing that in the [110] direction less of the misfit strain is taken up by the 90° dislocations. The width of the satellites in the [110] direction was larger than for the other orientation by approximately a factor of 2 suggesting that the dislocation array is less ordered in this direction.

The x-ray scattering from a thin sample, A, is also shown in figure 2. The position of the satellites along the $[1\bar{1}0]$ direction is 1.106(2) nm^{-1} and corresponds to a dislocation spacing of 5.681(10) nm. In contrast to the data for sample B, the widths of the satellites are largely independent of the order of the satellite. This is characteristic of the scattering from a finite length of the dislocation array, and the width of 0.08(1) nm^{-1} for the first-order satellites gives a correlation length for the array of 76.3 ± 9 nm. The corresponding scattering observed when the [110] direction was in the scattering plane had a wave vector of 1.024(3) nm^{-1} giving a dislocation spacing of 6.136(18) nm. The widths of the satellite peaks are larger than for the $[1\bar{1}0]$ direction and are 0.12(1) nm^{-1} for the first-order satellites and 0.24(2) nm^{-1} for the second-order ones. This is typical for linewidths resulting from cumulative disorder as opposed to finite-size effects, and the fluctuation in the dislocation position is 0.72 nm.

Further information about the misfit dislocations was obtained from scans of the wave-vector transfer along the q_z-direction while the q_x-component was fixed such that the scan passes through one of the satellite peaks. A typical result is shown in figure 3. There are two peaks centred at $q_z = 41.23(1)$ nm^{-1} and $q_z = 44.30(1)$ nm^{-1} which are the wave-vector components q_z of the GaSb and GaAs (004) Bragg reflections respectively. The intensities of the two peaks are similar and the widths of the peaks are 1.80 nm^{-1} for the GaSb peak and 2.01 nm^{-1} for the GaAs peak. These results show that both the GaAs and GaSb are distorted by the dislocations and that their distortions extend about 3.3 nm into both materials. Since there are similar distortions associated with the two materials the dislocations are located at the interface. This is in contrast to the conclusions of Mallard *et al* [9], who suggest that the initial stages of GaSb deposition may produce a commensurate, defect-free layer of approximately three or four monolayers (1.5 nm) before the lattice relaxation starts to occur by the nucleation of misfit dislocations at the epilayer surface, resulting in the creation of a number of islands of elastically relaxed GaSb. Our data show no evidence for such a layer and suggest that the misfit dislocations occur at the interface.

Further evidence that this scattering arises from a regular array of 90° dislocations was obtained by calculating the scattering from 90° dislocations using the expressions given in the appendix of Kaganer *et al* [16]. The scattering from the 90° dislocation array was calculated by assuming that the displacements of the atoms due to the array were the superpositions of the displacements from the individual dislocations. The ratios of the scattered intensities for the first and second satellites and for the first and third satellites were then calculated as 14.9 and 52 respectively. The corresponding ratios from the experimental intensities are 11 ± 2 and 38 ± 5. The calculations of the width of the scattering as the wave vector was varied along the growth direction through the satellite reflections gave 1.2 nm^{-1} whereas the experimental

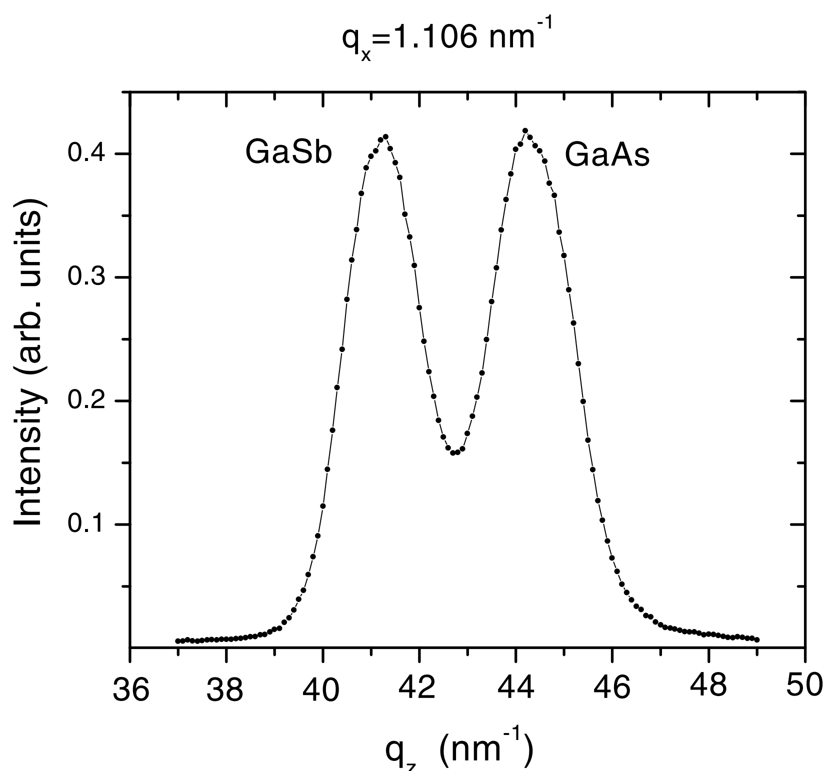

Figure 3. The x-ray scattering from sample A measured in a longitudinal scan through the first-order satellite shown in figure 2.

width, figure 3, is 1.8 nm^{-1}. These calculations show that a straightforward calculation of the scattering from the 90° dislocation array does produce a reasonably good description of the scattering, especially as the calculations assumed a rigid substrate whereas the results shown in figure 3 show that the GaAs substrate is distorted as well as the GaSb.

4. Islands and 60° misfit dislocations

The strong scattering from sample B near $q_x = 0$, figure 2, has an approximately Gaussian shape and the width increases from 0.036 nm^{-1} at (002) to 0.070 nm^{-1} at (004) and 0.104 nm^{-1} at (006). Since the width is increasing in proportion to the wave-vector transfer q_z, this scattering is characteristic of the scattering from a mosaic crystal with a mosaic spread of 0.098(5)°. When the sample is rotated such that the [110] direction is in the scattering plane, the width of the Gaussian peak for $q_x = 0$ corresponds to a mosaic spread of 0.19°, 1.9 times larger than when the [1$\bar{1}$0] direction is in the scattering plane.

The scattering centred around $q_x = 0$ for a thin sample, A, has very different structures for the two scattering planes as shown in figure 4. The scattering near the (002) Bragg reflection when the wave-vector transfer is along the [1$\bar{1}$0] direction shows a very sharp Gaussian peak centred on $q_x = 0$ and two broader Lorentzian peaks centred approximately at wave vectors of $q_x = \pm 0.027$ nm^{-1} and with a width of 0.039 nm^{-1}. The scattering around the (004) GaSb reflection is similar except that the width of the two displaced peaks increases to 0.053 nm^{-1}.

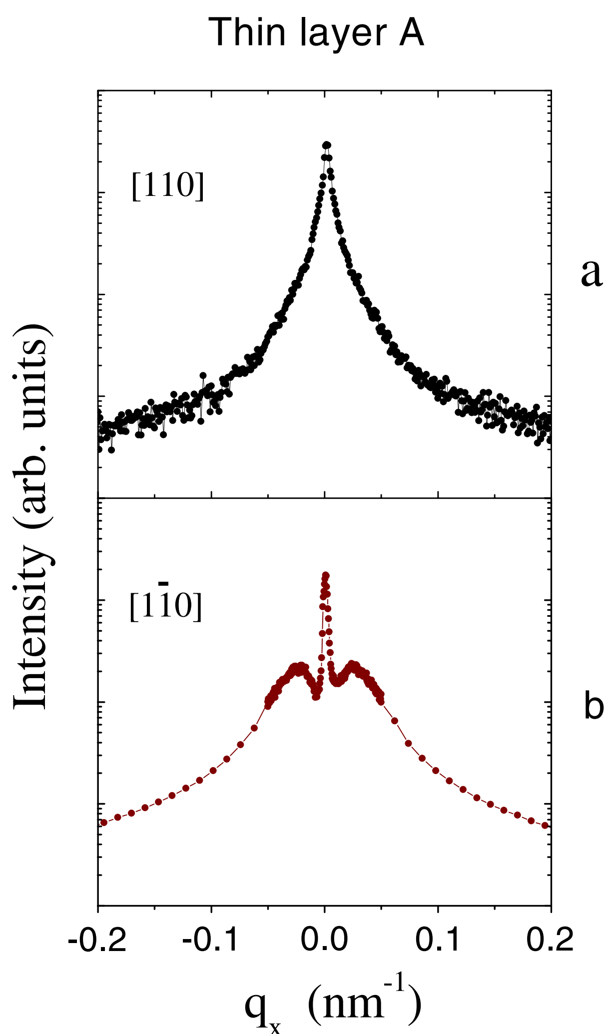

Figure 4. The x-ray scattering from a transverse scan through the (002) reflection of the GaSb layer, A. The wave vector is along [110] (a) and [1$\bar{1}$0] (b) directions.

In contrast, the scattering along the [110] direction shows a single peak, but detailed analysis shows that it can be reasonably described by two components: a Bragg-like sharp component and a broader component whose width is 0.027 nm^{-1} for (002) and 0.053 nm^{-1} for (004) reflections. A two-component line shape is frequently observed for epitaxial systems, but there is no universally accepted explanation and different mechanisms have been put forward to explain the two components [17–21].

Many features of the scattering in figure 4 can be understood. The sharp Bragg-like components from sample A arise from atomic planes that are on average flat over lengths of over 2.0×10^3 nm. Since AFM measurements, figure 1, show that a thin sample, A, has GaSb islands that are much smaller than this, the atomic planes in the different islands must scatter coherently, and consequently the structure of the islands must be quite perfect. The overall width of the broader scattering increases only slightly from the (002) through the (004) to the

(006) reflection. Consequently, this width does not arise from a mosaic structure as found for the thicker sample, but arises from the finite size of the islands. Since the approximate width of the scattering is 0.1 nm^{-1} in the [1$\bar{1}$0] direction and 0.05 nm^{-1} along [110], the average island size is about 63 nm along [1$\bar{1}$0] and 125 nm along the [110] direction. These estimates are consistent with the analysis of the widths of the 90° dislocation scattering described above and with the AFM results for [1$\bar{1}$0]. For the [110] direction the AFM measurements give a size substantially larger than 125 nm. Comparing the x-ray and AFM data one should bear in mind that the islands are trapezoidal, and that the base of each island is significantly bigger than the top (seen in the AFM image), and that the difference has a greater impact on the [1$\bar{1}$0] direction than on the [110] direction.

The displaced peaks shown in figure 4(b) are unusual. Peaks displaced from $q_x = 0$ can be formed by steps on the surface of the substrate [17] due to the difference in lattice parameter of the layer and the substrate producing a modulation in the atomic planes of the layer. The peaks shown in figure 4(b), however, contain most of the intensity of the scan and not just a very small fraction as found when they arise from steps. Consequently, the displaced peaks must arise from scattering from a large portion of the GaSb. We suggest that the displacements arise from islands containing one 60° misfit dislocation, and to investigate this we have calculated the scattering using the experiments given in the appendix of Kaganer *et al* [16].

The calculation of the scattered intensity due to the 60° dislocations is complex because they cause tilts as well as distortions of the layer. In agreement with the results obtained earlier [16], scattering from layers containing isolated 60° dislocations does have peaks at wave vectors corresponding to the average tilt of the material. Figure 4(b) shows peaks at wave vectors of 0.027 nm^{-1}, and if there was one dislocation in each island having a size of 70 nm the average tilt would correspond to a wave vector of 0.029 nm^{-1}. The results for the [110] direction, figure 4(a), do not have discrete peaks, possibly because the islands are larger and contain more than one 60° dislocation, which may then have different signs for the (001)-axis component of the Burgers vector.

5. Discussion

As we have shown above, the lattice mismatch between a GaSb layer and GaAs substrate is largely relaxed by 90° misfit dislocations arranged with a very regular period. This is consistent with the present understanding of dislocation formation in a variety of hetero-epitaxial systems. Comparison of the observed misfit dislocation structures shows that the dislocations are generally of the 60° type when the misfit strain is small (<2%), are of mixed 60° and 90° types for intermediate degrees of misfit and are predominantly of the Lomer 90° type for very large degrees of misfit (>6%) [9]. Nevertheless, the type of dislocation may depend on the growth conditions. Indeed, TEM and HREM measurements [4–6] have shown that lattice misfit relaxation mechanisms depend on the growth temperature. For a GaSb sample grown at 520 °C the lattice mismatch strain is accommodated mainly by 90° dislocations, but for a sample grown at 540 °C the misfit strain is relieved by both 90° and 60° dislocations, and for a sample grown at 560 °C the strain is accommodated mainly by 60° dislocations which cause a local tilt of the GaSb islands with respect to the GaAs substrate [5]. Our samples were grown at 520 °C and have mostly 90° dislocations in agreement with these results [5].

Our results are summarized in table 1. The spacing between the dislocations for both the [110] and [1$\bar{1}$0] directions decreases as the layer thickness increases, while the magnitude of the strain compared with that for bulk GaSb also decreases as the layer thickness increases. For both samples the structure of the layer is orthorhombic, with both lattice parameters in the (a, b) plane less than in the bulk while that along the growth direction, c, is increased. The magnitude

of the strain in the growth direction, table 1, is consistent with that reported for a sample grown by MBE [3, 13]. A large asymmetry in the residual in-plane strains and a large ratio (up to 1.2–1.8) of the densities of misfit dislocations for the [110] and $[1\bar{1}0]$ directions have been observed in some other systems which are mostly relaxed by 60°-type misfit dislocations—for example, in InGaAs/GaAs(001) [22–24], SiGe/Si(001) [25], $In_{1-x}Ga_xP$ and $GaAs_{1-x}P_x$ [26]. This asymmetry is related to the lattice asymmetry of the zinc-blende structure for orthogonal 60° dislocations of the same sign, leading to misfit dislocations being preferentially nucleated along the $[1\bar{1}0]$ direction [26]. We are uncertain of the origin of the asymmetry in our measurements with largely 90° dislocations.

In conclusion, we have made a detailed study of the structure of thin layers of GaSb grown on GaAs. The results show that the layers are orthorhombic in structure with a periodic modulation due to two intersecting arrays of 90° dislocations. The scattering shows that these dislocations are localized at the interface and that both the layer and substrate (a GaAs buffer layer) are distorted. The spacings of the dislocations are different along the [110] and $[1\bar{1}0]$ directions, showing that the 90° dislocations are less effective at removing the strain in the [110] direction. This is also the direction in which the islands grow largest and the direction in which the mosaic spread of the thick sample is largest. It is reasonable then to conclude that more of the strain in this direction is taken up by 60° dislocations than for the $[1\bar{1}0]$ direction.

This study illustrates the power of high-resolution x-ray scattering techniques for the study of lattice-mismatched materials. It enables a detailed study of the structure and of the dislocation networks.

Acknowledgments

The work was funded by the UK Engineering and Physical Sciences Research Council (EPSRC). This work was performed on the EPSRC-funded XMaS beamline at the ESRF. We are grateful to the beamline team for their invaluable assistance.

References

[1] Aindow M, Cheng T T, Mason N J, Seong T-Y and Walker P J 1993 *J. Cryst. Growth* **133** 168
[2] Rocher A *et al* 1991 *Microscopy of Semiconducting Materials 1991 (Inst. Phys. Conf. Ser. 117)* (Bristol: Institute of Physics Publishing) section 7, pp 509–14
[3] Qian W, Skowronski M and Kaspi R 1997 *J. Electrochem. Soc.* **144** 1430
[4] Kang J M, Nouaoura M, Lassabatere L and Rocher A 1994 *J. Cryst. Growth* **143** 115
[5] Kim J-H, Seong T-Y, Mason N J and Walker P J 1998 *J. Electron. Mater.* **27** 466
[6] Rocher A and Kang J M 1995 *Microscopy of Semiconducting Materials 1995 (Inst. Phys. Conf. Ser. 146)* (Bristol: Institute of Physics Publishing) pp 135–42
[7] Qian W, Skowronski M, Kaspi R, Graef M D and Dravid V P 1997 *J. Appl. Phys.* **81** 7268
[8] Rocher A M 1991 *Solid State Phenomena* vol 19–20 (Vaduz: Sci-Tech) pp 563–72
[9] Mallard R E, Wilshaw P R, Mason N J, Walker P J and Booker G R 1989 *Microscopy of Semiconducting Materials 1989 (Inst. Phys. Conf. Ser. 100)* (Bristol: Institute of Physics Publishing) section 4, pp 331–6
[10] Kang J M and Rocher A 1994 *Phil. Mag. Lett.* **70** 363
[11] Rocher A and Snoeck E 1998 *Thin Solid Films* **319** 172
[12] Rocher A M 1997 *Microscopy of Semiconducting Materials 1997 (Inst. Phys. Conf. Ser. 157)* (Bristol: Institute of Physics Publishing) pp 153–6
[13] Bourret A and Fuoss P H 1992 *Appl. Phys. Lett.* **61** 1034
[14] Booker G R *et al* 1997 *J. Cryst. Growth* **170** 777
[15] Fullerton E E, Schuller I K, Vanderstraeten H and Bruynseraede Y 1992 *Phys. Rev.* B **45** 9292
[16] Kaganer V M, Köhler R, Schmidbauer M R O R and Jenichen B 1997 *Phys. Rev.* B **55** 1793
[17] Gibaud A, Cowley R A, McMorrow D F, Ward R C C and Wells M R 1993 *Phys. Rev.* B **48** 14 463
[18] Reimer P, Zabel H, Flynn C P, Dura J A and Ritley K 1993 *Z. Phys. Chem.* **181** 375

[19] Farrow R F C *et al* 1993 *J. Cryst. Growth* **133** 47
[20] Huth M and Flynn C P 1997 *Appl. Phys. Lett.* **71** 2466
[21] Miceli P F, Palmstrom C J and Moyers K W 1991 *Appl. Phys. Lett.* **58** 1602
[22] Kavanagh K L, Chang J C P, Chen J, Fernandez J M and Wieder H H 1992 *J. Vac. Sci. Technol.* B **10** 1820
[23] Kavanagh K L *et al* 1998 *J. Appl. Phys.* **64** 4843
[24] Lazzarini L *et al* 1997 *Microscopy of Semiconducting Materials 1997 (Inst. Phys. Conf. Ser. 157)* (Bristol: Institute of Physics Publishing) pp 149–52
[25] Stiffler S R, Stanis C L, Goorsky M, Chan K K and de Fresart E 1992 *J. Appl. Phys.* **71** 4820
[26] Abrahams M S, Blanc J and Buiocchi C J 1972 *Appl. Phys. Lett.* **21** 185